Journal of
Applied & Computational Mathematics

Nowar et al., J Applied Computat Mathemat 2012, 1:2
DOI: 10.4172/2168-9679.1000102

Research Article | Open Access

Peristaltic Pumping of Johnson-Segalman Fluid in an Asymmetric Channel under the Effect of Hall and Ion-Slip Currents

Kh. Nowar[1]*, E. Abo-Eldahab[2] and E. Barakat[2]

[1]*Department of Mathematics, Faculty of Science, King Saud University, Riyadh, Saudia Arabia*
[2]*Department of Mathematics, Faculty of Science, Helwan University, Helwan, Egypt*

Abstract

The influences of Hall and ion-slip currents on peristaltic transport of Johnson-Segalman fluid in an asymmetric channel are investigated theoretically and graphically. The problem is formulated using a perturbation method. The solutions have been derived for axial velocity, axial pressure gradient and pressure rise. It has been noticed that the axial pressure gradient is not affected by increasing any of Hall or ion-slip parameters, while the time average flux decreases by increasing any of them. The effects of various emerging parameters on the axial pressure gradient and the pumping characteristics are discussed and plotted.

Keywords: Johnson-Segalman fluid; Hall currents; Ion-slip; Asymmetric channel; Peristalsis

Introduction

Peristaltic pumping is a special kind of transport, in which, physiological fluids may be pumped from one place in the body to another place. Peristaltic motion flows attracted the attention of many researchers because it is widely observed in industry and biology. Intense research on peristalsis has been done and is still demanded because of its useful applications. Such applications include enhanced oil recovery, chemical processes such as in distillation towers and fixed-bed reactors, urine transport from kidney to bladder through the ureter, transport of lymph in the lymphatic vessels, swallowing food through the esophagus, the movement of chyme in the gastrointestinal tract, ovum movement in the fallopian tube, transportation of spermatozoa in the ductus efferentes of the male reproductive tracts, in the vasomotion of small blood vessels, in sanitary fluid transport, and blood pumps in heart lung machine. In addition, peristaltic pumping occurs in many practical applications involving bio-mechanical systems. The peristaltic flows can be divided to Newtonian and non-Newtonian flows that have been reported analytically, numerically, and experimentally by a number of researchers [1-11]. Although most prior studies of peristaltic transport have focused on Newtonian fluids, there are also studies involving non-Newtonian fluids [12-20] i.e. fluids in which the relation between shear stress and shear rate is not linear.

The Johnson-Segalman fluid is one of the developed models to predict non-Newtonian effects. This model is a viscoelastic fluid model which was developed to allow for non-affine deformations [21]. Some investigations [22-24] have studied this model to explain the phenomenon of spurt. The term spurt is used to describe the large increase in the volume throughout for a small increase in the driving pressure gradient at a critical pressure gradient. Hayat et al. [16] examined the peristaltic flow of a magnetohydrodynamic Johnson-Segalmann fluid for planner channel and found the perturbation solutions and general solutions using symmetry method. Elshahed and Haroun [25] studied the peristaltic transport of Johnson-Segalman fluid under the effect of magnetic field. Haroun [26] considered the peristaltic flow of an inclined asymmetric channel for fourth grade fluid. Srinivas and Pushparaj [27] discussed the non-linear peristaltic transport in an inclined asymmetric channel. Hayat et al. [28] investigated the peristaltic transport of a Johnson-Segalman fluid in an asymmetric channel. Reddy and Raju [29] studied the non-linear peristaltic pumping of Johnson-Segalman fluid in an asymmetric channel under the effect of a magnetic field. Abo-Eldahab et al. [30-31] investigated the effects of Hall and ion-slip currents on magnetohydrodynamic peristaltic transport and couple stress fluid.

The aim of this paper is to investigate the effect of Hall and ion-slip currents on peristaltic transport of a Johnson-Segalman fluid in an asymmetric channel. We introduce the governing equations and boundary conditions as mentioned below. The perturbation solution for small Weissenberg number is mentioned below. Numerical results, discussions and conclusions are also mentioned below.

Problem Formulation

Consider the peristaltic flow of an incompressible Johnson-Segalman fluid in a two dimensional infinite asymmetric channel of width d_1+d_2. The asymmetry in the channel is produced by assuming the peristaltic wave train on the channel walls traveling with the same speed c but with different amplitudes and phases as shown in Figure 1; The walls of the channel are defined as

$$H_1(X,t) = d_1 + a_1\cos(\frac{2\pi}{\lambda}[X-ct]), \text{Upper} \quad \text{wall}, \quad (1)$$

$$H_2(X,t) = -d_2 - a_2\cos(\frac{2\pi}{\lambda}[X-ct]+\theta), \text{Lower} \quad \text{wall}, \quad (2)$$

Where a_1, a_2 are the amplitudes of the upper and lower waves, λ is the wave length, θ is the phase difference and t is the time. Note that $\theta = 0$ corresponds to an asymmetric channel with waves out of phase and $\theta = \pi$ describes the case where waves are in phase. Further, d_1, d_2, a_1, a_2, and θ satisfy the following inequality

***Corresponding author:** Kh. Nowar, Department of Mathematics, Faculty of Science, King Saud University, Riyadh, Saudia Arabia, E-mail: khalidnowar@yahoo.com

Received March 03, 2012; **Accepted** April 08, 2012; **Published** April 12, 2012

Citation: Nowar Kh, Abo-Eldahab E, Barakat E (2012) Peristaltic Pumping of Johnson-Segalman Fluid in an Asymmetric Channel under the Effect of Hall and Ion-Slip Currents. J Applied Computat Mathemat 1:102. doi:10.4172/2168-9679.1000102

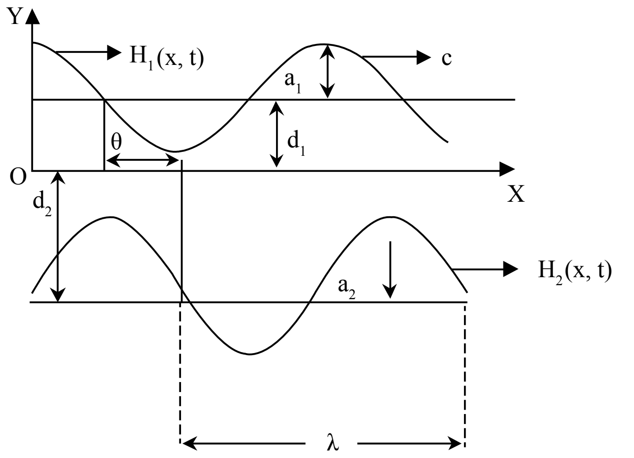

Figure 1: Geometry of the problem.

$$a_1^2 + a_2^2 + 2a_1a_2\cos\theta \le (d_1+d_2)^2 \quad (3)$$

so that the walls will not intersect with each other.

The fundamental equations governing the flow of an incompressible Johnson-Segalman fluid together with the generalized Ohm's law taking the effects of Hall and ion-slip currents, and Maxwell's equations into account are:

$$\nabla.V = 0 \quad (4)$$

$$\nabla.\tau + J \wedge B = \rho\frac{dV}{dt} \quad (5)$$

$$J = \frac{\sigma\alpha_e}{\alpha_e^2+\beta_e^2}(E + V\wedge B) - \frac{\sigma\beta_e}{\alpha_e^2+\beta_e^2}(E+V\wedge B)\wedge\frac{B}{B_0} \quad (6)$$

$$\nabla\wedge B = \mu_m J,\quad \nabla\wedge E = -\frac{\partial B}{\partial t},\quad \nabla.B = 0 \quad (7)$$

$$\tau = -P\mathbf{I} + 2\mu\mathbf{D} + \mathbf{S} \quad (8)$$

$$\mathbf{S} + m[\frac{d\mathbf{S}}{dt} + \mathbf{S}(\mathbf{W}-e\mathbf{D}) + (\mathbf{W}-e\mathbf{D})^T\mathbf{S}] = 2\eta\mathbf{D} \quad (9)$$

$$\mathbf{D} = \frac{1}{2}[\mathbf{L}+\mathbf{L}^T],\quad \mathbf{W} = \frac{1}{2}[\mathbf{L}-\mathbf{L}^T],\quad \mathbf{L} = grad\ \ \mathbf{V} \quad (10)$$

where,

V is the velocity vector, ρ is the density of the fluid, $\frac{d}{dt}$ is the material derivative, τ is the Cauchy stress tensor, J is the current density, B is the total magnetic field, E is the total electric field, σ is the electric conductivity, μm is the electric permeability, and $\alpha_e = 1+\beta_i\beta_e$, βi is the ion-slip parameter, and βe is the Hall parameter. Further, P is the pressure, μ and η are the dynamic viscosities, m is the relaxation time, e is the slip parameter and D, W are the symmetric and skew symmetric part of the velocity gradient, respectively. It should be noted that this model includes the viscous Navier-Stokes fluid as a special case for m = 0. Further, when e = 1 the Johnson-Segalman model reduces to the Oldroyd-B fluid; and when μ = 0 and e = 1, the model reduces to the Maxwell fluid. It is assumed that there is no applied or polarization voltage so that E = 0. Now we assume that a magnetic field $B = (0, 0, B_0)$ with a constant magnetic flux density B_0 is applied orthogonal to the channel. Neglecting the induced magnetic field under the assumption that the magnetic Reynolds number is small, we get from (6) that the magnetohydrodynamic force is

$$J\wedge B = \frac{\sigma B_0^2}{\alpha_e^2+\beta_e^2}[(\beta_e v - \alpha_e u)\mathbf{i} - (\alpha_e v - \beta_e u)\mathbf{j}] \quad (11)$$

Following Shapiro et al. [32] we introduce a wave frame of reference (x, y) moving with velocity c in which the motion becomes independent of time when the channel is an integral multiple of the wavelength and the pressure difference at the ends of the channel is a constant. The transformation from the fixed frame of reference (X, Y) to the wave frame of reference (x, y) is given by

$$x = X - ct,\quad y = Y,\quad u = U - c,\quad v = V,\quad \text{and}\quad p(x) = P(x,t) \quad (12)$$

Where (u, v), p and (U, V), P are the velocity components and pressure in the wave and fixed frames of reference respectively.

The governing equations in a wave frame of reference are given by

$$\frac{\partial u}{\partial x} + \frac{\partial v}{\partial y} = 0 \quad (13)$$

$$\rho(u\frac{\partial u}{\partial x} + v\frac{\partial u}{\partial y}) = -\frac{\partial p}{\partial x} + \mu(\frac{\partial^2 u}{\partial x^2} + \frac{\partial^2 u}{\partial y^2}) + \frac{\partial S_{xx}}{\partial x} + \frac{\partial S_{xy}}{\partial y} + \frac{\sigma B_0^2}{(\alpha_e^2+\beta_e^2)}[-\alpha_e(u+c) + \beta_e v](14)$$

$$\rho(u\frac{\partial v}{\partial x} + v\frac{\partial v}{\partial y}) = -\frac{\partial p}{\partial y} + \mu(\frac{\partial^2 v}{\partial x^2} + \frac{\partial^2 v}{\partial y^2}) + \frac{\partial S_{xy}}{\partial x} + \frac{\partial S_{yy}}{\partial y} - \frac{\sigma B_0^2}{(\alpha_e^2+\beta_e^2)}[\alpha_e v + \beta_e(u+c)](15)$$

$$2\eta\frac{\partial u}{\partial x} = S_{xx} + m[u\frac{\partial S_{xx}}{\partial x} + v\frac{\partial S_{xx}}{\partial y}] - 2emS_{xx}\frac{\partial u}{\partial x} + m[(1-e)\frac{\partial v}{\partial x} - (1+e)\frac{\partial u}{\partial y}]S_{xy} \quad (16)$$

$$\eta(\frac{\partial u}{\partial y} + \frac{\partial v}{\partial x}) = S_{xy} + m[u\frac{\partial S_{xy}}{\partial x} + v\frac{\partial S_{xy}}{\partial y}] + \frac{m}{2}[(1-e)\frac{\partial u}{\partial y} - (1+e)\frac{\partial v}{\partial x}]S_{xx}$$

$$+\frac{m}{2}[(1-e)\frac{\partial v}{\partial x} - (1+e)\frac{\partial u}{\partial y}]S_{yy} \quad (17)$$

$$2\eta\frac{\partial v}{\partial y} = S_{yy} + m[u\frac{\partial S_{yy}}{\partial x} + v\frac{\partial S_{yy}}{\partial y}] - 2emS_{yy}\frac{\partial v}{\partial y} + m[(1-e)\frac{\partial u}{\partial y} - (1+e)\frac{\partial v}{\partial x}]S_{xy} \quad (18)$$

Introducing the following non-dimensional variables

$$x^* = \frac{x}{\lambda},\quad y^* = \frac{y}{d_1},\quad u^* = \frac{u}{c},\quad v^* = \frac{v}{c\delta},\quad S^* = \frac{d_1}{\mu c}S, p^* = \frac{pd_1^2}{c\lambda(\mu+\eta)},\quad t^* = \frac{ct}{\lambda},$$

$$h_1 = \frac{H_1}{d_1},\quad h_2 = \frac{H_2}{d_1},\quad \delta = \frac{d_1}{\lambda},\quad R_e = \frac{\rho d_1 c}{\mu},\quad W_i = \frac{mc}{d_1},\quad d = \frac{d_2}{d_1},\quad \phi_1 = \frac{a_1}{d_1},$$

$$\phi_2 = \frac{a_2}{d_1},\quad M^2 = \frac{\sigma B_0^2 d_1^2\alpha_e}{\mu(\alpha_e^2+\beta_e^2)},\quad N^2 = \frac{\sigma B_0^2 d_1^2\beta_e}{\mu(\alpha_e^2+\beta_e^2)} \quad (19)$$

into equations (13)-(18) and dropping the stars we get;

$$\frac{\partial u}{\partial x} + \frac{\partial v}{\partial y} = 0 \quad (20)$$

$$\delta R_e(u\frac{\partial u}{\partial x} + v\frac{\partial u}{\partial y}) = -(\frac{\mu+\eta}{\mu})\frac{\partial p}{\partial x} + \delta^2\frac{\partial^2 u}{\partial x^2} + \frac{\partial^2 u}{\partial y^2} + \delta\frac{\partial S_{xx}}{\partial x} + \frac{\partial S_{xy}}{\partial y} - M^2(u+1) + N^2\delta v \quad (21)$$

$$\delta^3 R_e(u\frac{\partial v}{\partial x} + v\frac{\partial v}{\partial y}) = -(\frac{\mu+\eta}{\mu})\frac{\partial p}{\partial y} + \delta^4\frac{\partial^2 v}{\partial x^2} + \delta^2\frac{\partial^2 v}{\partial y^2} + \delta^2\frac{\partial S_{xy}}{\partial x} + \delta\frac{\partial S_{yy}}{\partial y}$$

$$-N^2\delta(u+1) - M^2\delta^2 v \quad (22)$$

$$\frac{2\delta\eta}{\mu}\frac{\partial u}{\partial x} = S_{xx} + \delta W_i(u\frac{\partial}{\partial x} + v\frac{\partial}{\partial y})S_{xx} - 2e\delta W_i S_{xx}\frac{\partial u}{\partial x} + W_i[\delta^2(1-e)\frac{\partial v}{\partial x} - (1+e)\frac{\partial u}{\partial y}]S_{xy} \quad (23)$$

$$\frac{\eta}{\mu}\left(\frac{\partial u}{\partial y}+\delta^2\frac{\partial v}{\partial x}\right)=S_{xy}+\delta W_i\left(u\frac{\partial}{\partial x}+v\frac{\partial}{\partial y}\right)S_{xy}+\frac{W_i}{2}\left[(1-e)\frac{\partial u}{\partial y}-(1+e)\delta^2\frac{\partial v}{\partial x}\right]S_{xx}$$

$$+\frac{W_i}{2}\left[(1-e)\delta^2\frac{\partial v}{\partial x}-(1+e)\frac{\partial u}{\partial y}\right]S_{yy} \quad (24)$$

$$\frac{2\delta\eta}{\mu}\frac{\partial v}{\partial y}=S_{yy}+W_i\delta\left(u\frac{\partial}{\partial x}+v\frac{\partial}{\partial y}\right)S_{yy}-2e\delta W_i S_{yy}\frac{\partial v}{\partial y}+W_i\left[(1-e)\frac{\partial u}{\partial y}-(1+e)\delta^2\frac{\partial v}{\partial x}\right]S_{xy} \quad (25)$$

Assuming that the wavelength is long and since the Reynolds number is low, then the equations (21)-(25) become

$$-\left(\frac{\mu+\eta}{\mu}\right)\frac{\partial p}{\partial x}+\frac{\partial^2 u}{\partial y^2}+\frac{\partial S_{xy}}{\partial y}-M^2(u+1)=0 \quad (26)$$

$$-\left(\frac{\mu+\eta}{\mu}\right)\frac{\partial p}{\partial y}=0 \quad (27)$$

$$S_{xx}=W_i(1+e)\frac{\partial u}{\partial y}S_{xy} \quad (28)$$

$$\frac{\eta}{\mu}\frac{\partial u}{\partial y}=S_{xy}+\frac{W_i}{2}(1-e)\frac{\partial u}{\partial y}S_{xx}-\frac{W_i}{2}(1+e)\frac{\partial u}{\partial y}S_{yy} \quad (29)$$

$$S_{yy}=-W_i(1-e)\frac{\partial u}{\partial y}S_{xy} \quad (30)$$

Using (28) and (30) in (29) we get

$$S_{xy}=\frac{\eta}{\mu}\left[\frac{\partial u}{\partial y}-W_i^2(1-e^2)\left(\frac{\partial u}{\partial y}\right)^3\right] \quad (31)$$

From (26) and (31) we can get

$$\frac{\partial^2 u}{\partial y^2}-\alpha W_i^2\frac{\partial}{\partial y}\left(\frac{\partial u}{\partial y}\right)^3-K^2u=K^2+\frac{dp}{dx} \quad (32)$$

where

$$\alpha=\frac{\Gamma}{\Gamma+1},\quad \Gamma=\frac{\eta}{\mu},\quad K^2=\frac{M^2}{1+\Gamma} \quad (33)$$

The corresponding boundary conditions are

$$u=-1 \quad \text{at} \quad y=h_1,\quad u=-1 \quad \text{at} \quad y=h_2 \quad (34)$$

where

$$h_1=1+\phi_1\cos 2\pi x \quad (35)$$

and

$$h_2=-d-\phi_2\cos(2\pi x+\theta) \quad (36)$$

Rate Of Volume Flow

The volume flow rate in wave frame of reference is given by

$$q=\int_{h_2(x)}^{h_1(x)}u(x,y)dy \quad (37)$$

where h_1, h_2 are functions of x alone.

The instantaneous volume flow rate in the fixed frame is given by

$$Q=\int_{h_2(x,t)}^{h_1(x,t)}[u(x,y,t)+1]dy=q+h_1-h_2 \quad (38)$$

in which h_1, h_2 are functions of x and t.

The time-mean flow over time period $T=\lambda/c$ is given by

$$\bar{Q}(x,t)=\frac{1}{T}\int_0^T Q(x,y)dt=\frac{1}{T}\int_0^T(q+h_1-h_2)dt=q+1+d \quad (39)$$

Method Of Solution

It is not possible to get an exact solution for equation (32) because, it is a nonlinear differential equation, so we focus our attention to find analytical solution by using the perturbation method. By expanding the flow quantities in a power series of the small parameter W_i^2 as follows:

$$u=u_0+W_i^2u_1+O(W_i^4) \quad (40)$$

$$\frac{dp}{dx}=\frac{dp_0}{dx}+W_i^2\frac{dp_1}{dx}+O(W_i^4) \quad (41)$$

$$q=q_0+W_i^2q_1+O(W_i^4) \quad (42)$$

Substituting from (40)-(42) into (32) and (34) and collecting terms according to powers of W_i and identifying the coefficients of like powers of W_i we obtain the following systems.

Zeroth-order system (W_i^0)

$$\frac{d^2u_0}{dy^2}-K^2u_0=K^2+\frac{dp}{dx} \quad (43)$$

The corresponding boundary conditions are

$$u_0=-1 \quad \text{at} \quad y=h_1,\quad u_0=-1 \quad \text{at} \quad y=h_2 \quad (44)$$

First-order system (W_i^2)

$$\frac{d^2u_1}{dy^2}-\alpha\frac{\partial}{\partial y}\left(\frac{\partial u_0}{\partial y}\right)^3-K^2u_1=\frac{dp_1}{dx} \quad (45)$$

The corresponding boundary conditions are

$u1 = 0$ at $y = h1$, $u1 = 0$ at $y = h_2$ (46)

Zeroth-order solution

The general solution of (43) can be easily obtained in the form

$$u_0=\frac{1}{K^2}\frac{dp_0}{dx}[A_1\cosh Ky+A_2\sinh Ky-1]-1 \quad (47)$$

By using (44) we find that the constants A_1 and A_2 take the forms

$$A_1=\frac{\sinh Kh_2-\sinh Kh_1}{\sinh K(h_2-h_1)},\quad A_2=\frac{\cosh Kh_1-\cosh Kh_2}{\sinh K(h_2-h_1)} \quad (48)$$

The volume flow rate q_0 is given by

$$q_0=\int_{h_2}^{h^1}u_0dy$$

$$=\frac{1}{K^3}\frac{dp_0}{dx}\left[\frac{2-2\cosh K(h_1-h_2)-K(h_1-h_2)\sinh K(h_2-h_1)}{\sinh K(h_2-h_1)}\right]-(h_1-h_2) \quad (49)$$

From (49) we can write

$$\frac{dp_0}{dx}=\frac{K^3(q_0+(h_1-h_2))\sinh K(h_2-h_1)}{2-2\cosh K(h_1-h_2)-K(h_1-h_2)\sinh K(h_2-h_1)} \quad (50)$$

Citation: Nowar Kh, Abo-Eldahab E, Barakat E (2012) Peristaltic Pumping of Johnson-Segalman Fluid in an Asymmetric Channel under the Effect of Hall and Ion-Slip Currents. J Applied Computat Mathemat 1:102. doi:10.4172/2168-9679.1000102

First-order solution

Substituting from (47) into (45) and solving (45) we get

$$u_1 = \frac{1}{K^2}\frac{dp_1}{dx}[A_1\cosh Ky + A_2\sinh Ky - 1] +$$

$$\frac{3\alpha}{8K^4}\left(\frac{dp_0}{dx}\right)^3[g(y) - A_3\cosh Ky - A_4\sinh Ky] \quad (51)$$

where

$$A_3 = \frac{g(h_1)\sinh Kh_2 - g(h_2)\sinh Kh_1}{\sinh K(h_2-h_1)} \quad (52)$$

$$A_4 = \frac{g(h_2)\cosh Kh_1 - g(h_1)\cosh Kh_2}{\sinh K(h_2-h_1)} \quad (53)$$

$$g(y) = S_1\cosh 3Ky + S_2\sinh 3Ky + 4S_3Ky\sinh Ky + 4S_4Ky\cosh Ky \quad (54)$$

$$S_1 = \frac{1}{4}(A_1^3 + 3A_1A_2^2) \quad , \quad S_2 = \frac{1}{4}(A_2^3 + 3A_1^2A_2) \quad (55)$$

$$S_3 = \frac{1}{4}(-A_1^3 + A_1A_2^2) \quad , \quad S_4 = \frac{1}{4}(3A_2^3 + 5A_1^2A_2) \quad (56)$$

the volume flow rate is given by

$$q_1 = \int_{h_2}^{h^1} u_1 dy$$

$$= \frac{1}{K^3}\frac{dp_1}{dx}\left[\frac{2-2\cosh K(h_1-h_2) - K(h_1-h_2)\sinh K(h_2-h_1)}{\sinh K(h_2-h_1)}\right]$$

$$+\frac{3\alpha}{8K^4}\left(\frac{dp_0}{dx}\right)^3 A_5 \quad (57)$$

and,

$$A_5 = \frac{S_1}{3K}(\sinh 3Kh_1 - \sinh 3Kh_2) + \frac{S_2}{3K}(\cosh 3Kh_1 - \cosh 3Kh_2)$$

$$+\frac{4S_3}{K}(Kh_1\cosh Kh_1 - \sinh Kh_1 - Kh_2\cosh Kh_2 + \sinh Kh_2)$$

$$+\frac{4S_4}{K}(Kh_1\sinh Kh_1 - \cosh Kh_1 - Kh_2\sinh Kh_2 + \cosh Kh_2)$$

$$-\frac{A_3}{K}(\sinh Kh_1 - \sinh Kh_2) - \frac{A_4}{K}(\cosh Kh_1 - \cosh Kh_2) \quad (58)$$

From (57) we can obtain

$$\frac{dp_1}{dx} = \frac{K^3\sinh K(h_2-h_1)[q_1 - \frac{3\alpha}{8K^4}(\frac{dp_0}{dx})^3 A_5]}{2-2\cosh K(h_1-h_2) - K(h_1-h_2)\sinh K(h_2-h_1)} \quad (59)$$

substituting from (50) and (59) into (41), taking (42) into account, and neglecting terms of $O(W_i^4)$ we get

$$\frac{dp}{dx} = \frac{K^3\sinh K(h_2-h_1)[q+h_1-h_2]}{2-2\cosh K(h_1-h_2) - K(h_1-h_2)\sinh K(h_2-h_1)}$$

$$-\frac{\frac{3\alpha}{8}W_i^2 A_5 K^8 (q_0+h_1-h_2)^3\sinh^4 K(h_2-h_1)}{[2-2\cosh K(h_1-h_2) - K(h_1-h_2)\sinh K(h_2-h_1)]^4} \quad (60)$$

The dimensionless pressure rise per one wavelength in the wave frame is defined as

$$\Delta p = \int_0^1 \left(\frac{\partial p}{\partial x}\right) dx \quad (61)$$

Results and Discussion

This section represents the graphical results in order to be able to discuss the quantitative effects of the sundry parameters involved in the analysis.

The variation of the axial pressure gradient $\frac{dp}{dx}$ with x for various values of W_i, Γ, β_e, and β_i are shown in Figure 2. Figure (2a) studies the effects of Weissenberg number W_1 on the axial pressure gradient $\frac{dp}{dx}$, and it is noticed that the axial pressure gradient increases by increasing Weissenberg number. Further it is observed that the axial pressure gradient is more for Johnson-Segalman fluid ($0 < W_i < 1$) than that of Newtonian fluid ($W_i = 0$). Figure (2b) shows the variation of the axial pressure gradient $\frac{dp}{dx}$ with viscosity ratio Γ. It is clear that the axial pressure gradient increases with an increase in viscosity ratio. In Figures (2c) and (2d) it is obvious that the axial pressure gradient has not affected by increasing the Hall and ion-slip parameters.

Figure 3 illustrates the variation of the axial pressure gradient $\frac{dp}{dx}$ with x for different values of θ, φ_1, φ_2 and d. It is clear that the axial

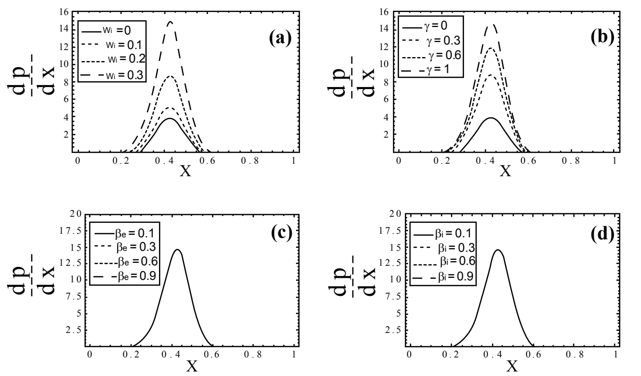

Figure 2: The variation of the axial pressure gradient $\frac{dp}{dx}$ with x for various values of Weissenberg number W_i (panel a), viscosity ratio Γ (panel b), Hall parameter β_e (panel c), and ion-slip parameter β_i (panel d). The other parameters chosen are:
$B_0 = 0.8, d_1 = 0.9, \Gamma = 1, \mu = 1, \sigma = 0.7, d = 1.2, \theta = \frac{\pi}{4}, \beta_e = 0.2, \beta_i = 0.3, \phi_1 = 0.5, \phi_2 = 0.7$ (panel a);
$B_0 = 0.8, d_1 = 0.9, W_i = 0.3, \mu = 1, \sigma = 0.7, d = 1.2, \theta = \frac{\pi}{4}, \beta_e = 0.2, \beta_i = 0.3, \phi_1 = 0.5, \phi_2 = 0.7$ (panel b);
$B_0 = 0.8, d_1 = 0.9, W_i = 0.3, \mu = 1, \sigma = 0.7, d = 1.2, \Gamma = 1, \theta = \frac{\pi}{4}, \beta_i = 0.3, \phi_1 = 0.5, \phi_2 = 0.7$ (panel c);
$B_0 = 0.8, d_1 = 0.9, W_i = 0.3, \mu = 1, \sigma = 0.7, d = 1.2, \Gamma = 1, \theta = \frac{\pi}{4}, \beta_e = 0.2, \phi_1 = 0.5, \phi_2 = 0.7$

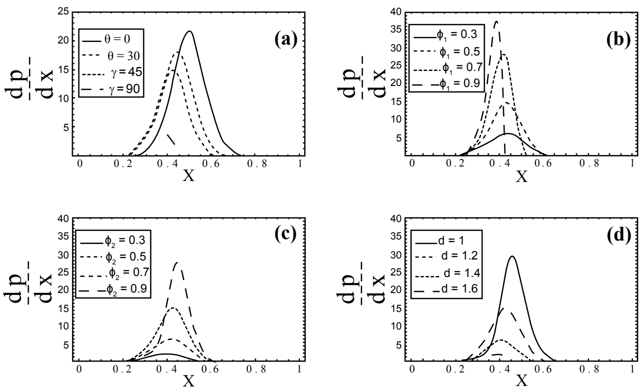

Figure 3: The variation of the axial pressure gradient $\frac{dp}{dx}$ with for various values of phase shift θ (panel a), upper wave amplitude ϕ_1 (panel b), lower wave amplitude ϕ_2 (panel c), and width of the channel d (panel d). The other parameters chosen are:

$B_0 = 0.8, d_1 = 0.9, \Gamma = 1, \mu = 1, \sigma = 0.7, d = 1.2, W_i = 0.3, \beta_e = 0.2, \beta_i = 0.3, \phi_1 = 0.5, \phi_2 = 0.7$ (panel a);

$B_0 = 0.8, d_1 = 0.9, W_i = 0.3, \mu = 1, \sigma = 0.7, d = 1.2, \theta = \frac{\pi}{4}, \beta_e = 0.2, \beta_i = 0.3, \Gamma = 1, \phi_2 = 0.7$ (panel b);

$B_0 = 0.8, d_1 = 0.9, W_i = 0.3, \mu = 1, \sigma = 0.7, d = 1.2, \Gamma = 1, \theta = \frac{\pi}{4}, \beta_i = 0.3, \phi_1 = 0.5, \beta_e = 0.2$ (panel c);

$B_0 = 0.8, d_1 = 0.9, W_i = 0.3, \mu = 1, \sigma = 0.7, \beta_i = 0.3, \Gamma = 1, \theta = \frac{\pi}{4}, \beta_e = 0.2, \phi_1 = 0.5, \phi_2 = 0.7$ (panel d).

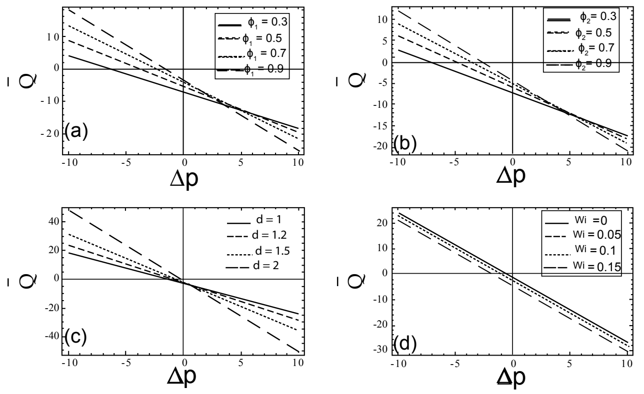

Figure 5: The variation of time average flux $\bar{Q}$ with Δp for different values of upper wave amplitude ϕ_1 (panel a), lower wave amplitude ϕ_2 (panel b), width of the channel d (panel c), and Weissenberg number W_i (panel d). The other parameters chosen are:

$B_0 = 0.8, d_1 = 0.9, W_i = 0.3, \mu = 1, \sigma = 0.7, d = 1.2, \theta = \frac{\pi}{4}, \beta_e = 0.2, \beta_i = 0.3, \Gamma = 1, \phi_2 = 0.7$ (panel a);

$B_0 = 0.8, d_1 = 0.9, W_i = 0.3, \mu = 1, \sigma = 0.7, d = 1.2, \Gamma = 1, \theta = \frac{\pi}{4}, \beta_i = 0.3, \phi_1 = 0.5, \beta_e = 0.2$ (panel b);

$B_0 = 0.8, d_1 = 0.9, W_i = 0.3, \mu = 1, \sigma = 0.7, \beta_i = 0.3, \Gamma = 1, \theta = \frac{\pi}{4}, \beta_e = 0.2, \phi_1 = 0.5, \phi_2 = 0.7$ (panel c);

$B_0 = 0.8, d_1 = 0.9, \Gamma = 1, \mu = 1, \sigma = 0.7, d = 1.2, \theta = \frac{\pi}{4}, \beta_e = 0.2, \beta_i = 0.3, \phi_1 = 0.5, \phi_2 = 0.7$ (panel d).

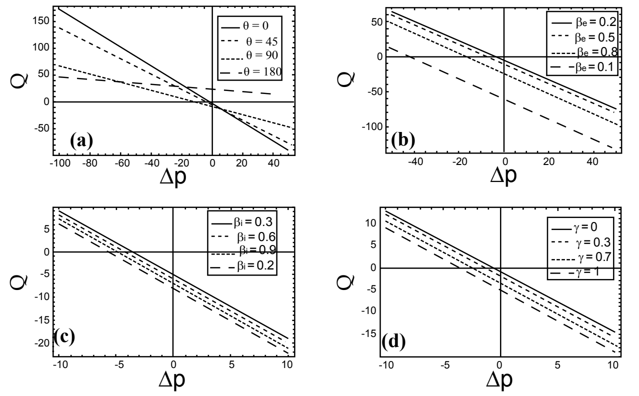

Figure 4: The variation of time average flux $\bar{Q}$ with Δp for different values of phase shift θ (panel a), Hall parameter β_e (panel b), ion-slip parameter β_i (panel c), and viscosity ratio Γ (panel d). The other parameters chosen are:

$B_0 = 0.8, d_1 = 0.9, \Gamma = 1, \mu = 1, \sigma = 0.7, d = 1.2, W_i = 0.3, \beta_e = 0.2, \beta_i = 0.3, \phi_1 = 0.5, \phi_2 = 0.7$ (panel a);

$B_0 = 0.8, d_1 = 0.9, W_i = 0.3, \mu = 1, \sigma = 0.7, d = 1.2, \theta = \frac{\pi}{4}, \phi_1 = 0.5, \beta_i = 0.3, \Gamma = 1, \phi_2 = 0.7$ (panel b);

$B_0 = 0.8, d_1 = 0.9, W_i = 0.3, \mu = 1, \sigma = 0.7, d = 1.2, \Gamma = 1, \theta = \frac{\pi}{4}, \beta_e = 0.2, \phi_1 = 0.5, \phi_2 = 0.7$ (panel c);

$B_0 = 0.8, d_1 = 0.9, W_i = 0.3, \mu = 1, \sigma = 0.7, \beta_i = 0.3, d = 1.2, \theta = \frac{\pi}{4}, \beta_e = 0.2, \phi_1 = 0.5, \phi_2 = 0.7$

pressure gradient decreases by increasing the phase shift θ (Figure (3a)), and also decreases by increasing the width of the channel d (Figure (3d)). The situation is reversed in Figures (3b) and (3c), the axial pressure gradient is increased with an increase in φ_1 and φ_2.

In Figure 4 we studied the variation of time average flux $\bar{Q}$ with Δp for different values of θ, β_e, β_i and Γ. Figure (4a) declares that the time average flux $\bar{Q}$ decreases by increasing the phase shift θ in both co-pumping ($\Delta p < 0$) and free pumping ($\Delta p = 0$), while it increases by increasing the phase shift θ in the pumping region ($\Delta p > 0$). Figures (4b), (4c), (4d) reveal that, the time average flux $\bar{Q}$ decreases by increasing the Hall parameter β_e (Figure (4b)), the ion-slip parameter β_i (Figure (4c)), and the viscosity ratio Γ (Figure (4d)) in each of the three regions.

Figure 5 considered the variation of time average flux $\bar{Q}$ with Δp for different values of φ_1 φ_2, d, and W_i. It is obvious from Figures (5a), (5b), and (5c) that the time average flux increases by increasing φ_1, φ_2, and d in the co-pumping and free pumping regions, also it decreases by increasing them in the pumping region. The variation of time average flux $\bar{Q}$ with Δp for different values of Weissenberg number W_i studied in Figure (5d), and it is observed that the time average flux decreases by increasing Weissenberg number in each of the three regions.

Conclusions

In the present paper, the effects of Hall and ion-slip currents on the peristaltic transport of a Johnson-Segalman fluid in an asymmetric channel under assumptions of a constant external magnetic field, low Reynolds number, and long wavelength are investigated. The governing equations are first modeled and then solved analytically. The effects of various emerging parameters on the axial pressure gradient and time average flux are observed from the graphs. The results are summarized as follows:

The axial pressure gradient $\frac{dp}{dx}$ increases by increasing any of Weissenberg number W_i, viscosity ratio Γ, and upper or lower wave amplitudes φ_1 *or* φ_2.

The axial pressure gradient $\frac{dp}{dx}$ is not affected by increasing any of

Hall or ion-slip parameters β_e and β_i

Increasing the phase shift θ or the width of the channel d decreases the axial pressure gradient.

The time average flux $\bar{Q}$ decreases by increasing any of Hall parameter β_e, ion-slip parameter β_i, viscosity ratio Γ, and Weissenberg number W_i.

An increase in the phase shift θ decreases the time average flux $\bar{Q}$ in the co-pumping and free pumping regions and increases it in the pumping region.

The time average flux $\bar{Q}$ increases by increasing any of upper or lower wave amplitude (φ_1 or φ_2), and the width of the channel d in the co-pumping and free pumping regions and it decreases by increasing them in the pumping region.

References

1. Pozrikidis CA (1987) A study of peristaltic flow. J Fluid Mech 180: 515-527.
2. Osnat E, David E (1999) Analysis of intra-uterine fluid motion induced by uterine contractions. Bull Math Biol 61: 221-238.
3. Ali N, Hussain Q, Hayat T, Asghar S (2008) Slip effects on peristaltic transport of MHD fluid with variable viscosity. Phys Lett A 372: 1477-1489.
4. Mekheimer KhS, Elshehawey EF, Alaw M (1998) Peristaltic motion of a particle-fluid suspension in a planner channel. Int J Theory Phys 37: 2895-2920.
5. Mekheimer KhS (2002) Peristaltic transport of a couple stress fluid in a uniform and non-uniform channels. Biorheology 39: 755-765.
6. Naby AEHAE, Misery AEME, Shamy IIE (2003) Hydromagnetic flow of fluid with variable viscosity in uniform tube with peristalsis, J Phys A: Math Gen 36: 8535.
7. Hayat T, Ali N, Ashgar S, Siddiqui AM (2006) Exact peristaltic flow in tubes with an endoscope. Appl Math Comput 182: 359-368.
8. Mekheimer KhS (2003) Non-linear Peristaltic transport of magneto-hydrodynamic flow in an inclined planner channels. Arab J Sci Eng 28: 183-201.
9. Mekheimer KhS (2004) Peristaltic flow of blood under the effect of magnetic field in a non-uniform channels. Appl Math Comput 153: 763-777.
10. Siddiqui AM, Hayat T, Khan M (2004) Magnetic fluid model induced by peristaltic waves. J Phys Soc Jpn 73: 2142-2147.
11. Naby AEHAE, Misery AEME, Kareem MFAE (2006) Effects of a magnetic field on trapping through peristaltic motion for generalized Newtonian fluid in channel. Physica A 367: 79-92.
12. Hayat T, Javed M, Ali N (2008) MHD Peristaltic transport of a Jeffery fluid in a channel with compliant walls and porous space. Transp Porous Med 74: 259-274.
13. Srivastava LM, Srivastava VP (1984) Peristaltic transport of blood: Casson model-II. J Biomech 17: 821-829.
14. Hayat T, Wang Y, Siddiqui AM, Ashgar S (2004) A mathematical model for study of gliding motion of bacteria on a layer of non-Newtonian slime. Math Method Appl Sci 27: 1447-1468.
15. Hayat T, Wang Y, Siddiqui AM, Hutter K, Ashgar S (2002) Peristaltic transport of a third order fluid in a circular cylindrical tube. Math Models Methods Appl Sci 12: 1691-1706.
16. Hayat T, Wang Y, Siddiqui AM, Hutter K (2003) Peristaltic motion of a Johnson-Segalman fluid in a planner channel. Math Probl Eng 1: 1-23.
17. Hayat T, Mahomed FM, Ashgar S (2005) Peristaltic flow of a magnetohydrodynamic Johnson-Segalman fluid. Nonlinear Dynamics 40: 375-385.
18. Haroun MH (2005) Effect of relaxation and retardation time on peristaltic transport of the Oldroydian viscoelastic fluid. Journal of Applied Mechanics and Technical Physics 46: 842-850.
19. Mishra M, Rao AR (2003) Peristaltic transport of a Newtonian fluid in asymmetric channel. Z angew Math Phys 54: 532-550.
20. Rao AR, Mishra M (2004) Non-linear and curvature effects on peristaltic flow of a viscous fluid in an asymmetric channel. Acta Mech 16: 835-59.
21. Johnson Jr MW and Segalman D (1977) A model for viscoelastic fluid behavior which allows non-affine deformation, J Nonnewton. Fluid Mech 2: 255-270.
22. Kolkka RW, Malkus DS, Hansen MG, Ierley GR (1988) Spurt phenomenon of the Johnson-Segalman fluid and related models. J Nonnewton Fluid Mech 29: 303-335.
23. Malkus DS, Nohel JA, Plohr BJ (1990) Dynamics of shear flow of non-Newtonian fluid. J Comput Phys 87: 464-487.
24. McLeish TCB, Ball RC (1986) A molecular approach to the spurt effect in polymer melt flow. J Polym Sci B Polym Phys 24: 1735-1745.
25. Elshahed M, Haroun MH (2005) Peristaltic transport of Johnson-Segalman fluid under effect of a magnetic field. Mathematical Problems in Engineering 6: 663-677.
26. Haroun MH (2007) Non-linear peristaltic flow of a fourth grade fluid in an inclined asymmetric channel. Computational Materials Science 39: 324 -333.
27. Srinivas S, Pushparaj V (2008) Non-linear peristaltic transport in an inclined asymmetric channel. Commun Nonlinear Sci Numer Simul 13: 1782-1795.
28. Hayat T, Ambreen A, Ali N (2008) Peristaltic transport of a Johnson-Segalman fluid in an asymmetric channel. Math Comput Model 47: 380-400.
29. Reddy MS, Raju GSS (2010) Non-linear peristaltic pumping of Johnson-Segalman fluid in an asymmetric channel under the effect of a magnetic field. European J. os scientific research 1: 147-164.
30. Abo-Eldahab EM, Barakat EI, Nowar Kh (2010) Hall currents and ion-slip effects on the MHD peristaltic transport. Int J Appl Math Phys 2: 113-123.
31. Abo-Eldahab EM, Barakat EI, Nowar Kh (2010) Effects of Hall and ion-slip currents on peristaltic transport of a couple stress fluid. Int J Appl Math Phys 2: 145 -157.
32. Shapiro AH, Jaffrin MY, Weinberg SL (1969) Peristaltic pumping with long wavelengths at low Reynolds number. J Fluid Mech 37: 799-825.